Jurnal Ilmu Fisika
Vol. 16, No. 1, March 2024, pp. 22–33
ISSN: 1979-4657 (Print); 2614-7386 (Online)
https://doi.org/10.25077/jif.16.1.22-33.2024

Jurnal Ilmu Fisika
Open Access

Efficiency at Maximum Power of Endoreversible Quantum Otto Engine with Partial Thermalization in 3D Harmonic Potential

Zahara Zettira[1], Trengginas E. P. Sutantyo[1*], Zulfi Abdullah[1]
[1]Theoretical Physics Laboratory, Department of Physics, Faculty of Mathematics and Natural Sciences, Universitas Andalas, Limau Manis, Padang, 25163, Indonesia

Article Info

Article History:

Received August 3, 2023
Revised September 18, 2023
Accepted September 19, 2023
Published online September 22, 2023

Keywords:

Partial thermalization
Bose-Einstein Condensate
Quantum Otto Engine
Efficiency at maximum power
Entropy production

Corresponding Author:

Trengginas E. P. Sutantyo,
Email:
trengginasekaputra@sci.unand.ac.id

ABSTRACT

We study the partial thermalization to the effect of efficiency at maximum power (EMP) of a quantum Otto engine using Bose-Einstein Condensation in 3D harmonic potential. Partial thermalization occurs at a finite-time isochoric process, preventing the medium from achieving equilibrium with reservoirs, leaving it in a state of residual coherence. Under these circumstances, the performance of the engine can be seen from its power and EMP. The 3D harmonic potential is used to generate an excitation of energy during the expansion and compression. The total energy is defined by the total work done in a cycle. Using Fourier's law in conduction, we found that power explicitly depends on the duration of heating and cooling stroke time and efficiency of the engine; that is the higher stroke time and efficiency, the less power output. In order to find EMP, we maximize power with respect to compression ratio κ, and we found that EMP also depends on the isochoric heating and cooling process. By varying the stroke time of the isochoric process, EMP slightly decreases with increasing isochoric time due to entropy production. However, adjusting cooling stroke time more extended than heating stroke time could significantly improve the EMP of Otto Engine.

1. INTRODUCTION

The existence of quantum theory has a significant impact on other classical theories, including thermodynamics. Applying quantum theory in thermodynamics is also known as quantum thermodynamics (Deffner & Campbell, 2019). One of the most fascinating studies in this field is the Quantum Heat Engine (QHE), spearheaded by Scovil and Dubois in 1959 (Scovil & Schulz-Dubois, 1959). QHE is a device that uses quantum material as a working substance in order to convert heat into practical work. Some types of QHE operate similarly to classical engines (Abah et al., 2012; Deffner, 2018; Smith et al., 2020), but some are very different (Kim et al., 2022; Myers, Abah, et al., 2022; Myers, Peña, et al., 2022). The main motivation is to create a more practical and efficient engine model as close to the realistic engine.

The highest efficiency is bounded by Carnot efficiency, but this engine operates slowly, which causes zero power output. In an ideal Carnot cycle, all the processes are reversible, causing no entropy production to occur during the cycle. Reversible processes are impossible in the real world because friction will always occur during the cycle, which makes the cycle irreversible and reduces efficiency. Curzon-Ahlborn (1975) resolved this problem by applying endoreversible thermodynamics to the

classical Carnot engine; as a result, the power output is non-zero, but the endoreversible efficiency is less than the quasistatic efficiency. However, one found that (Scully et al., 2003) replacing classical material with quantum material as a working substance could enhance the efficiency of the engine (Fahriza et al., 2022; Fahriza & Sutantyo, 2022). By using quantum material, there has been a great deal of research on this endoreversible approach using various thermodynamics cycles, starting from Carnot cycle (Altintas, 2019; Dann & Kosloff, 2020; Niedenzu et al., 2018; Sutantyo et al., 2015), Lenoir cycle (Fahriza et al., 2022; Shen et al., 2017; Wang et al., 2021), Otto cycle (Boubakour et al., 2022; B. Çakmak & Müstecaplloğlu, 2019; Fei et al., 2022; Jiao et al., 2021; Myers, Peña, et al., 2022; Peña et al., 2023; Zettira et al., 2023), and Stirling cycle (Kaushik & Kumar, 2000; Yin et al., 2020). Nevertheless, instead of implementing other cycles, the Otto cycle is receiving significant attention since it is frequently used in practical engines. This widespread adoption is primarily due to the Otto cycle's exceptional efficiency, versatility, and compatibility with various engine types, making it a preferred choice for a wide range of vehicles. Moreover, advancements in engineering and technology continue to enhance the performance and efficiency of Otto engine, which is this study's primary motivation.

The main difference between an endoreversible Otto cycle and a quasistatic Otto cycle is in the thermalization process. In the quasistatic cycle, thermal contact between medium and reservoirs is extended long enough, making thermal equilibrium achievable. Meanwhile, in the endoreversible cycle, the thermal contact is speeded up so that the medium never reaches thermal equilibrium with the reservoir. In the previous study (Deffner, 2018; Kosloff & Rezek, 2017; Myers, Peña, et al., 2022; Smith et al., 2020; Zettira et al., 2023), it has been found that the efficiency of the endoreversible Otto engine using classical materials is exactly Curzon-Ahlborn efficiency and independent of external potential acting on it. However, efficiency using quantum materials such as Bose-Einstein Condensate (BEC) is significantly higher than Curzon-Ahlborn efficiency and highly depends on applied external potential. Moreover, the engine efficiency with BEC also depends on thermal contact between the hot and cold reservoirs (Camati et al., 2019; Chand et al., 2021; Zettira et al., 2023). Nevertheless, in that study, the effect of thermalization was only carried out on theoretical linear potentials. Here, we utilize a harmonic potential, which is commonly used in the experimental realization of BEC, due to the critical temperature of the BEC phase is achievable, i.e., nano Kelvin (nK) orde (Aveline et al., 2020). Thus, the harmonic potential proves to be more applicable than the linear potential.

In this study, we examine the quantum Otto engine efficiency at maximum power with BEC as a working medium trapped in the 3D harmonic potential. The cycle is treated endoreversibly, in which compression and expansion stroke are adiabatic quasistatic, while heating and cooling stroke is not quasistatic, meaning the working substance never reaches equilibrium with the reservoir. The power produced in a cycle is visualized as a function of efficiency. In order to find the efficiency at maximum power (EMP), we maximize the power numerically with respect to compression ratio κ. We found that EMP is highly dependent on heating (τ_h) and cooling (τ_l) stroke time and varying both will significantly affect the EMP. The imbalance time stroke of the cycle will intrigue partial thermalization, which is by setting an appropriate value of τ_h and τ_l, could improve EMP more significantly, and this is the main focus of this study. By using Otto cycle that only consists of adiabatic and isochoric stroke, we can easily generate the situation of partial thermalization by focusing the investigation on the isochoric only since the adiabatic is treated in a quasistatic manner. Furthermore, by deriving the formula in a 3D harmonic potential state, the physical properties' clarity can be implemented in future studies rather than the lower dimension state, especially for experiments or even on a prototype quantum engine.

2. FORMALISM OF ENDOREVERSIBLE QUANTUM OTTO ENGINE

2.1 Thermodynamics Property of BEC in 3D Harmonic Potential

In this study, we use N-number of bosons in the regime Bose-Einstein Condensate (BEC) as the working substance of the quantum Otto engine. BEC trapped in 3-dimensional harmonic potential. Using the Schrödinger equation, we can get the energy eigenvalue of the system. This energy eigenvalue can be linked to other thermodynamic quantities such as internal energy and entropy. Internal energy

and entropy are essential parameters to find the amount of work, power, and efficiency of an engine. As referred to (Griffiths & Schroeter, 2018; Pathria & Beale, 2011; Zettili & Zahed, 2003), the harmonic potential has a form.

$$V(\mathbf{r}) = \frac{1}{2} m\omega^2 \left(x^2 + y^2 + z^2 \right). \tag{1}$$

The change of energy through excitation is the work produced in the cycle. However, using the Schrödinger equation to find the energy eigenvalue in a system containing the N-number of particles is challenging. Despite this, boson in a condensate state experiences the same quantum state, making the ground state energy must be degenerate. But in this case, due to $k_B T \gg \varepsilon_{i+1} - \varepsilon_i$, so that the degeneracy is replaced with a density of state $D(\varepsilon)$, which in the 3D harmonic potential based on Eq. (1) has the form (Pathria & Beale, 2011),

$$D(\varepsilon) = \frac{\varepsilon^2}{(\hbar\omega)^3}. \tag{2}$$

In order to find the thermodynamic properties of BEC under 3D harmonic potential, we need to apply the density of state to the grand canonical potential (Ω) in Bose-Einstein statistic (Pitaevskii & Lev, 2016). The formulation of grand canonical potential for the bosonic system is formulated as

$$\Omega = k_B T \int_0^\infty D(\varepsilon) \ln\left(1 - z e^{-\beta\varepsilon}\right) d\varepsilon. \tag{3}$$

We have $z = e^{\frac{\mu}{k_B T}}$ as fugacity and $\beta = 1/k_B T$ as inverse thermal energy. By integrating Eq. (3), we get the formulation of grand canonical potential,

$$\Omega = -\frac{(k_B T)^4}{(\hbar\omega)^3} g_4(z) \tag{4}$$

with $g_4(z)$ is the Bose function defined as below

$$g_p(z) = \frac{1}{\Gamma(p)} \int_0^\infty \frac{x^{p-1}}{z^{-1} e^x - 1} dx, \tag{5}$$

where $\Gamma(p)$ is the gamma function. For discrete quantity, the Bose function can also be expanded in series form as follows (Pathria and Beale, 2011),

$$g_p(z) = \sum_{n=1}^{\infty} \frac{z^n}{n^p}. \tag{6}$$

As mentioned before, other thermodynamic properties can be derived directly from equation (4) using the relation $\Omega = U - TS - \mu N$ (Pathria and Beale, 2011). We obtained the entropy of BEC under 3D harmonic potential by deriving eq. (4) with respect to the T, written as

$$S(\omega, T) = 4k_B \left(\frac{k_B T}{\hbar\omega} \right)^3 \zeta(4). \tag{7}$$

Since BEC occurs when fugacity, z reaches its maximum value of 1, the Bose function when $z = 1$ can be replaced by zeta function, $\zeta(p)$. The phase transition to BEC occurs at a specific temperature, namely the critical temperature. The critical temperature of BEC depends on the number of particles, the type of trapping potential and the mass of bosons (Myers, Peña, et al., 2022; Pitaevskii, Lev, 2016; Reppy et al., 2000). By deriving eq. (4) with respect to μ, we get the critical temperature of BEC under 3D harmonic potential,

$$T_c = \frac{\hbar\omega}{k_B}\left(\frac{N}{\zeta(3)}\right)^{\frac{1}{3}}. \tag{8}$$

When the system reaches the critical temperature, all bosons do not immediately occupy the ground state but gradually occupy it as the temperature decreases. The fraction of bosons that remain in unoccupied state can be defined by eq. (8) (Myers, Peña, et al., 2022)

$$N_T = \left(\frac{k_B T}{\hbar\omega}\right)^3 g_3(z). \tag{9}$$

Another essential thermodynamics quantity to be determined is the internal energy. By substituting Eq. (4), (7), and (9) to the relation $\Omega = U - TS - \mu N$, we get the internal energy of BEC in 3D harmonic potential as below,

$$U(\omega,T) = 3k_B T\left(\frac{k_B T}{\hbar\omega}\right)^3 \zeta(4). \tag{10}$$

All of this quantity will be applied to the Otto cycle in order to find the power and efficiency of the Otto engine; we will discuss this in the following subsection.

2.2 Endoreversible Quantum Otto Engine

The Otto cycle consists of four strokes: isochoric heating (1-4), isentropic expansion (3-4), isochoric cooling (3-2), and isentropic compression (2-1). In the classical Otto engine, expansion and compression are carried out by moving the piston. Unlike in the quantum Otto engine, expansion and compression are done by varying the external field (Kosloff & Rezek, 2017), which is the inverse of the volume. During the isochoric stroke, the field is held constant, and the system is enabled to contact reservoirs. Meanwhile, in isentropic stroke the field is varied, but the system is isolated from the reservoirs. The process in each cycle is represented in Figure 1. The transition phase to BEC occurs at a specific critical temperature, which in the previous study (Aveline et al., 2020; Myers, Peña, et al., 2022; Zettira et al., 2023) is about 42 nK. Because of this, the temperature of the hot and cold reservoirs is assumed to be around this value in all simulations.

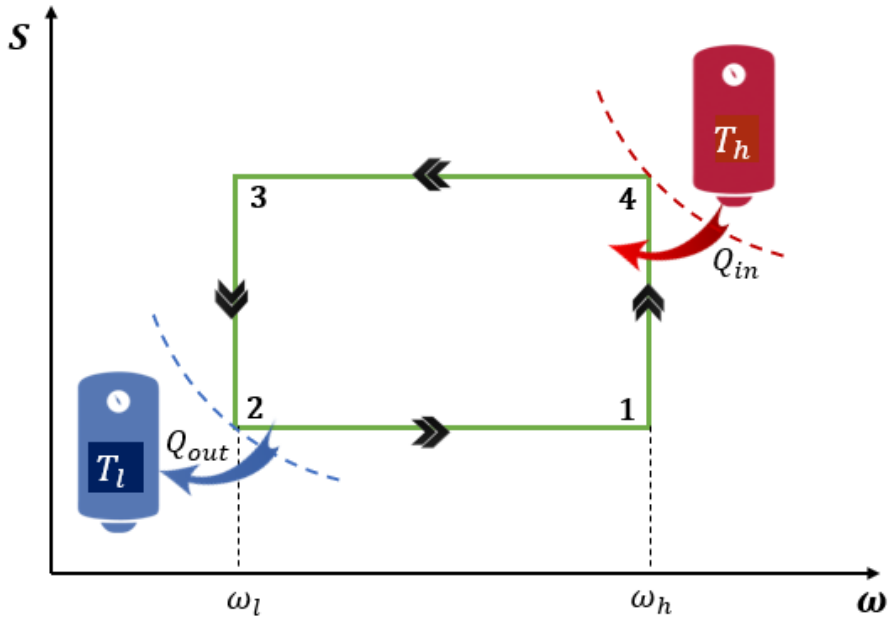

Figure 1. Endoreversible Otto cycle

The fundamental difference between quasistatic and endoreversible cycles is in the isochoric stroke. In an endoreversible cycle, the working substance never reaches equilibrium with reservoirs due to finite time. To link the temperature of the working substance and reservoir, we used Fourier's law for conduction (Deffner, 2018; Myers, Peña, et al., 2022). The amount of work and heat during each process are discussed below.

Isentropic expansion

During isentropic expansion, the working medium is isolated from the reservoir, and the external field is varied from ω_h to ω_l. The heat exchange during this process is zero because the working medium is isolated from reservoirs. Entropy also remains constant during the isentropic process, that is $S(\omega_l, T_3) = S(\omega_h, T_4)$ and $S(\omega_l, T_2) = S(\omega_h, T_1)$. By applying this relation to the eq. (7), we get the correlation of ω and T during the isentropic process.

$$T_2 = \frac{\omega_l}{\omega_h} T_1 = \kappa T_1 \quad \text{and} \quad T_4 = \frac{\omega_l}{\omega_h} T_3 = \kappa T_3 , \tag{11}$$

where κ is the compression ratio. Additionally, the amount of work during this process is $W_{exp} = U(\omega_l, T_3) - U(\omega_h, T_4)$. Using the relation of ω and T from eq. (11), we get the formulation of work during isentropic expansion,

$$W_{\exp} = \frac{3k_B^4 \zeta(4)(\kappa - 1)}{\omega_h^3 \hbar^3 \kappa^4 \left(e^{\alpha_h \tau_h + \alpha_l \tau_l} - 1\right)^4} \left\{ \left[T_l e^{\alpha_h \tau_h} \left(e^{\alpha_l \tau_l} - 1\right) + T_h \kappa \left(e^{\alpha_h \tau_h} - 1\right) \right]^4 \right\} . \tag{12}$$

Isochoric heating

In isochoric heating, medium contact with the hot reservoir while the external field is kept constant at ω_h, so the work during the heating process is zero. From the first law of thermodynamic, the amount of heat transferred to the medium is $Q_{in} = U(\omega_h, T_4) - U(\omega_h, T_1)$. As mentioned above, the temperature at the end of heating process is not equal to the hot reservoir (T_h), because the thermal time is finite, the change of temperature during the heating process can be described as (Deffner, 2018),

$$\frac{dT}{dt} = -\alpha_h \left(T - T_h\right), \tag{13}$$

with α_h is a constant that determines the heat capacity and thermal conductivity of the BEC in heating process. Using the boundary condition at the start and the end of a heating process, we get $T(0) = T_1$ and $T(\tau_h) = T_4$, where τ_h is the heating stroke time. Solving eq. (11) and apply those boundary conditions, we get the temperature difference during the heating process,

$$T_4 - T_h = \left(T_1 - T_h\right) e^{-\alpha_h \tau_h} . \tag{14}$$

Using Eq. (10), (11), and (14), we find the general formulation of heat transferred to the medium during the heating process.

$$Q_{in} = \frac{3k_B^4 \zeta(4)}{\omega_h^3 \hbar^3 \kappa^4 \left(e^{\alpha_h \tau_h + \alpha_l \tau_l} - 1\right)^4} \left\{ \left[T_l \left(e^{\alpha_l \tau_l} - 1\right) + T_h \kappa e^{\alpha_l \tau_l} \left(e^{\alpha_h \tau_h} - 1\right) \right]^4 - \left[T_l e^{\alpha_h \tau_h} \left(e^{\alpha_l \tau_l} - 1\right) + T_h \kappa \left(e^{\alpha_h \tau_h} - 1\right) \right]^4 \right\}$$

,

(15)

Isentropic compression

The medium is isolated again from the reservoir during isentropic compression, while the external field is varied from ω_l to ω_h. The amount of work is defined by the relation,

$W_{comp} = U(\omega_l, T_2) - U(\omega_l, T_3)$. Similar to isentropic expansion, by using eq. (11), we get the formulation of work during isentropic compression,

$$W_{comp} = \frac{3k_B^4\zeta(4)(1-\kappa)}{\omega_h^3\hbar^3\kappa^4\left(e^{\alpha_h\tau_h+\alpha_l\tau_l}-1\right)^4}\left[T_h\kappa e^{\alpha_l\tau_l}\left(e^{\alpha_h\tau_h}-1\right)+T_l\left(e^{\alpha_l\tau_l}-1\right)\right]^4. \quad (16)$$

Isochoric cooling

Medium contact with cold reservoir while the external field is kept constant at ω_l during isochoric cooling. The heat released to the cold reservoir causes the temperature of medium drops. The change of temperature during isochoric cooling can be determined by Fourier's law of conduction,

$$\frac{dT}{dt} = -\alpha_l\left(T - T_l\right), \quad (17)$$

where α_l is a constant that determines the heat capacity and thermal conductivity of the BEC in the cooling process. According to the boundary condition at the initial and the final cooling process, we get $T(0) = T_3$ and $T(\tau_l) = T_2$. Where τ_l is the cooling stroke time. Solving eq. (11) and apply those boundary conditions, we get the temperature difference during the cooling process,

$$T_2 - T_1 = \left(T_3 - T_1\right)e^{-\alpha_l\tau_l}. \quad (18)$$

With the same idea as isochoric heating, substitute Eq. (10), (11), and (18) to the amount of heat injected into the cold reservoir, $Q_{out} = U(\omega_l, T_2) - U(\omega_l, T_3)$, we get,

$$Q_{out} = \frac{3k_B^4\zeta(4)}{\omega_l^3\hbar^3\left(e^{\alpha_h\tau_h+\alpha_l\tau_l}-1\right)^4}\left\{\left[T_h\kappa e^{\alpha_l\tau_l}\left(e^{\alpha_h\tau_h}-1\right)+T_l\left(e^{\alpha_l\tau_l}-1\right)\right]^4-\left[T_l e^{\alpha_h\tau_h}\left(e^{\alpha_l\tau_l}-1\right)+T_h\kappa\left(e^{\alpha_h\tau_h}-1\right)\right]^4\right\}$$

(19)

2.3 Power and Efficiency

Power, *P* is the total work produced during a cycle divided by the total time during the cycle. The total time in a cycle is the summation of time in the isochoric and isentropic processes. As referred to references (Deffner, 2018; Kosloff & Rezek, 2017), the power produced in a cycle is formulated below,

$$P = -\frac{W_{\exp} + W_{comp}}{\gamma\left(\tau_l + \tau_h\right)}. \quad (20)$$

Where γ is the time multiplication constant. Using Equation (12) and (16), we get the power during one cycle as below,

$$P = \frac{3k_B^4\zeta(4)(1-\kappa)}{\omega_h^3\hbar^3\kappa^4\gamma\left(\tau_l+\tau_h\right)\left(e^{\alpha_h\tau_h+\alpha_l\tau_l}-1\right)^4}\left\{\left[T_h\kappa e^{\alpha_l\tau_l}\left(e^{\alpha_h\tau_h}-1\right)+T_l\left(e^{\alpha_l\tau_l}-1\right)\right]^4-\left[T_l e^{\alpha_h\tau_h}\left(e^{\alpha_l\tau_l}-1\right)+T_h\kappa\left(e^{\alpha_h\tau_h}-1\right)\right]^4\right\}$$

.

(21)

Efficiency is the fraction of work produced in a cycle to the amount of heat transferred to a working substance. The total work produced in a cycle is the summation of work in expansion and compression. The general formulation of efficiency is defined as (Deffner, 2018; Kosloff & Rezek, 2017),

$$\eta = -\frac{W_{exp} + W_{comp}}{Q_{in}}. \quad (22)$$

The higher the efficiency, the more heat can be converted into work. Substitute Eq. (12), (15), and (16) to Eq. (22), we get the formulation of efficiency Otto engine,

$$\eta = 1 - \kappa . \tag{23}$$

where $\kappa = \frac{\omega_l}{\omega_h}$ is a compression ratio. We see that efficiency only depends on the compression ratio and not on other physical properties of medium.

3. RESULTS AND DISCUSSION

Based on Equation (16), besides the dependency of the temperature of the reservoir, power also depends on the compression ratio and the time during the isochoric process. Due to the dominator in Eq. (16), the longer the cycle, the less power is produced. Whereas the efficiency does not depend on isochoric stroke time, so the efficiency of a quasistatic cycle and an endoreversible cycle will give the same formulation. (Zettira et al., 2023). However, high efficiency does not always produce high power; the highest efficiency is bounded by the Carnot limit, that is when $\eta = 1 - \frac{T_l}{T_h}$. If we substitute this relation to Eq. (21), we get power vanish at Carnot limit, making it impossible to achieve that efficiency in the practical world. This is the crucial reason to find the optimum efficiency, namely the Efficiency at Maximum Power (EMP), which is the efficiency when power reaches its maximum value. EMP is obtained by deriving Eq. (21) with respect to κ written as,

$$\left(\frac{\partial P}{\partial \kappa}\right)_{\kappa_{max}} = 0 . \tag{24}$$

In this derivation, we kept τ_l and τ_h constant. The aim is to see how EMP changes under the variation of these two parameters. Then κ_{max} is substituted back to Eq. (23) to get the efficiency at maximum compression ratio or EMP. The visualization of EMP is displayed in Figure 2.

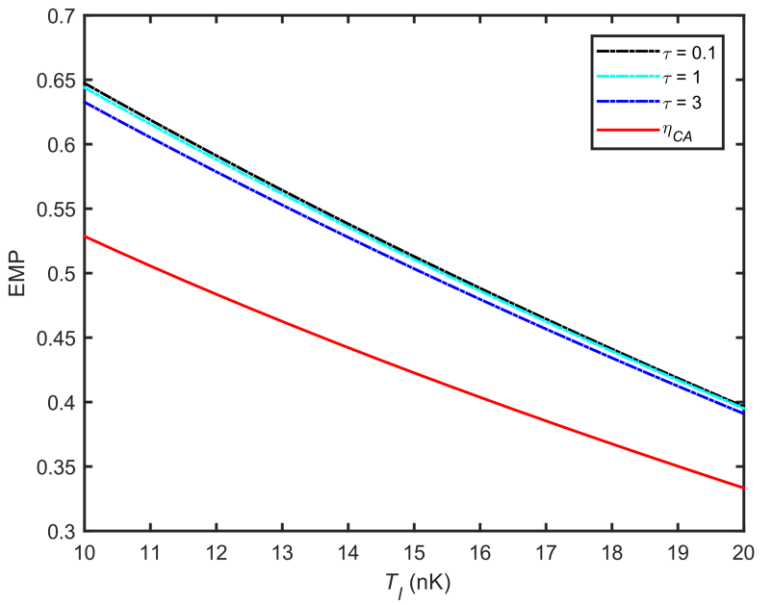

Figure 2. EMP as a function of T_l in variation of $\tau_l = \tau_h = \tau$ for 0.1; 1; 3 unit in time dimension, together with Curzon-Ahlborn efficiency (red-solid) as a comparison. The temperature of the hot reservoir is $T_h = 45$ nK.

It needs to be noted that the critical temperature of BEC in harmonic potential is approximately 42 nK based on previous studies (Myers, Peña, et al., 2022; Zettira et al., 2023); therefore, the hot and

cold reservoir temperatures we used have matched by this value. In Figure 2, we vary τ_l and τ_h at the same value, we see that EMP is slightly decrease as τ increase. This result is in agreement with (Zettira et al., 2023). Because of the dependency of power with isochoric stroke time in the denominator of Eq. (21), power will decrease as well τ_l and τ_h increase, the efficiency at this maximum power will also decrease. The reduce efficiency at raising isochoric time is caused by increasing entropy production. The more entropy production, the more irreversible the cycle; this irreversibility impacts reducing efficiency (S. Çakmak et al., 2017). However, during the cooling process the entropy will decrease, thereby balancing the entropy production during the heating process. This indicates that the decrease in EMP in Figure 2 is insignificant because the change in total entropy for a cycle is also insignificant. Moreover, increasing the entropy during heating is not precisely equal to decreasing the entropy during cooling (Camati et al., 2019) because the process is irreversible. The entropy production during isochoric heating can be defined by substituting the Eq. (14) to the Eq. (7), as formulated below

$$\Delta S_{4-1} = 4k_B\left(\frac{k_B}{\hbar\omega_h}\right)^3 \zeta(4)\left[\left(\left(T_1 - T_h\right)e^{-\alpha_h\tau_h} + T_h\right)^3 - T_1^3\right]. \tag{25}$$

While we set the temperature at the start of isochoric heating (T_1) to be constant because we want to explore the change of entropy when the temperature of the medium increases. The same method to find the entropy production during isochoric cooling by substituting Eq. (18) to Eq. (7), we get the change of entropy during the cooling process as follow,

$$\Delta S_{2-3} = 4k_B\left(\frac{k_B}{\hbar\omega_l}\right)^3 \zeta(4)\left[\left(\left(T_3 - T_l\right)e^{-\alpha_l\tau_l} + T_l\right)^3 - T_3^3\right]. \tag{26}$$

For visualization, we set the temperature at the start of isochoric cooling (T_3) to be constant, then we represent the visualization of Eq. (25) and (26) in Figure 3, which is the red line for the heating process (Figure 3.*a*) and the blue line for the cooling process (Figure 3.*b*).

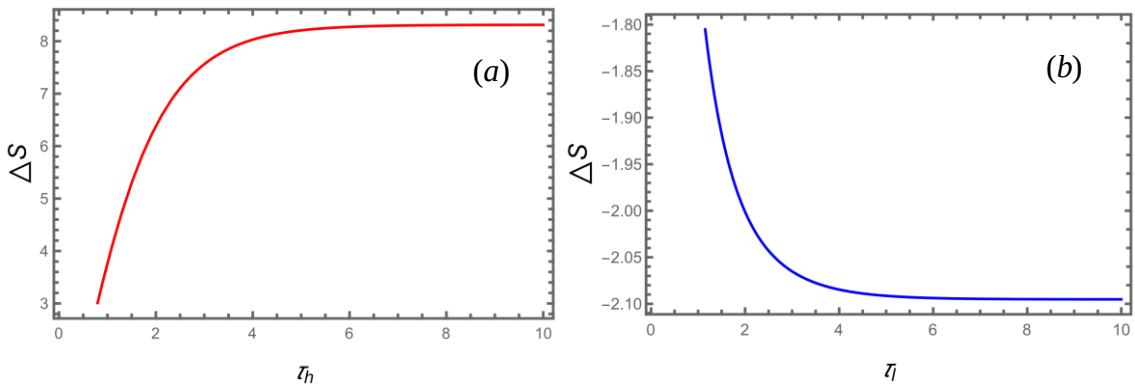

Figure 3. The change of entropy during (*a*) the heating process as a function of τ_h and (*b*) the change of entropy during the cooling process as a function τ_l. The temperature of reservoirs are $T_h = 45$ nK and $T_l = 20$ nK

Figure 3 shows that entropy increases with heating stroke time and decreases with cooling stroke time but will reach a saturation state when reaching thermal equilibrium. The rapid increase in entropy production at the beginning of the heating stroke creates quantum friction, reducing efficiency (Camati et al., 2019). However, varying the heating and cooling stroke time with different values can significantly improve EMP. In Figure 4, we visualize EMP with the different values of τ_l and τ_h. As we can see from Figure 4, EMP is significantly declining even close to Curzon-Ahlborn efficiency at long heating stroke times, but improving at long cooling stroke times. Adding cooling time continuously does not always result in a meaningful change in EMP. It proves by Figure 4.*a*, EMP at $\tau_l = 1$ almost the same as $\tau_l = 3$. This is related to the production of entropy during the heating and cooling strokes as

shown in Figure 3. Entropy production during heating and cooling strokes is a quantum signature of the system, which means it depends on intrinsic properties of the system, different mediums will experience different behaviour in the production entropy (Dann and Kosloff, 2020). Entropy production can also be linked to the coherence effect (Chand et al., 2021). In the case of partial thermalizations, this entropy production boosts EMP through residual coherence. Coherence in BEC is associated with the simultaneous collapse of each atom's wave function in the lowest quantum state, forming a single, macroscopic wave (Donley et al., 2008). The more atoms condensed into the ground state, the more coherent the wave function will be. The number of atoms in the condensate state depends on temperature. According to Eq. (8), the closer to the critical temperature, the fewer atoms are in the condensed state, and the highest condensate occurs at 0 K. Increasing the heating time will make the atoms excited from the ground state so that the fraction of atoms in the condensate decreases, which also causes a decrease in coherence and EMP. Conversely, increasing the cooling time will make the atoms descend to the ground state, increasing the coherence and the EMP. In order to optimize efficiency, the heating and cooling stroke time should be different, which means the heating stroke time must be slightly shorter than the cooling stroke time.

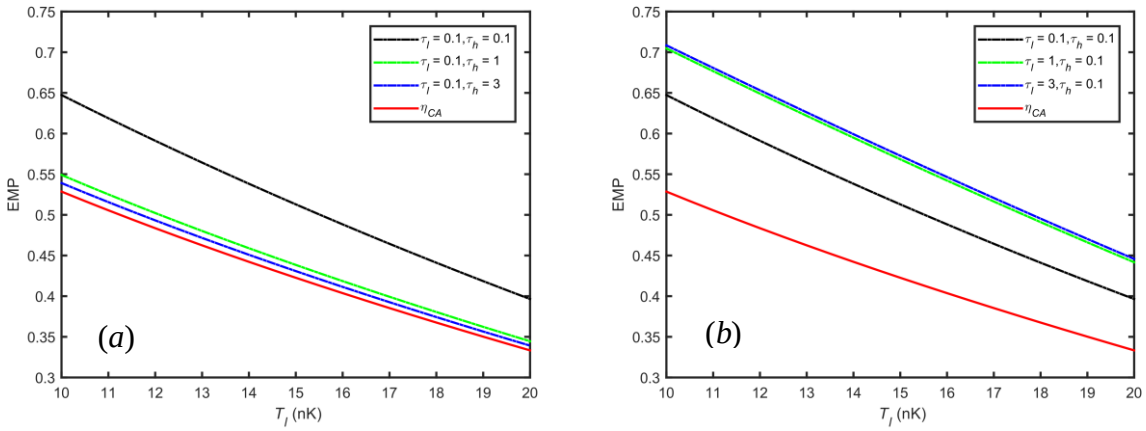

Figure 4. EMP as a function of T_l (*a*) at constant τ_l and (*b*) at constant τ_h together with Curzon-Ahlborn efficiency (red-solid) as a comparison. The temperature of hot reservoir is $T_h = 45$ nK.

Nevertheless, higher efficiency does not guarantee a higher power output. Efficiency is maximized at long and slow processes, producing no entropy during the cycle. Friction also vanishes at slow expansion and compression, making the cycle completely ideal and reversible. However, power descent to zero at a long and slow process. To prove that, we simulate the power dimensionless (P^*) as a function of efficiency in Figure 5. We modify Eq. (21) by replacing κ with $1-\eta$ from Eq. (23), which we get the formulation of P^*

$$P^* = \frac{1}{(\tau_l+\tau_h)\left(e^{\tau_h+\tau_l}-1\right)^4}\left\{\left[T_h e^{\tau_l}\left(e^{\tau_h}-1\right)+(1-\eta)^{-1}T_l\left(e^{\tau_l}-1\right)\right]^4-\left[(1-\eta)^{-1}T_l\left(e^{\tau_l}-1\right)+T_h\left(e^{\tau_h}-1\right)\right]^4\right\} \quad (27)$$

Here we use $\alpha_l = \alpha_h = 1$, and other parameters are based on Figure 4. To get the comparison, the τ_l and τ_h values are selected from the green line in Figure 4. In order to simplify the notation, let assume that when the cycle operates at $\tau_l = 1$, $\tau_h = 0.1$ is denoted by case A, and when the cycle operates at $\tau_l = 0.1$, $\tau_h = 1$ is denoted by case B. The maximum efficiency of A is attained at a lower efficiency than B, but the maximum power of A is significantly higher than B. This is because power is generated by the fraction of atoms outside the condensate (Myers et al., 2022b). For the case of ideal Bose gas, atoms in a condensed state (BEC) cannot generate or receive work because their compressibility are infinite (Pathria and Beale, 2011); therefore, work can only be done by the fraction

of atoms outside the condensate because their compressibility values are still finite. The greater the number of excited atoms, the greater the amount of work that can be produced. As previously stated, the fraction of excited atoms is temperature dependent; the higher the temperature approaches the critical

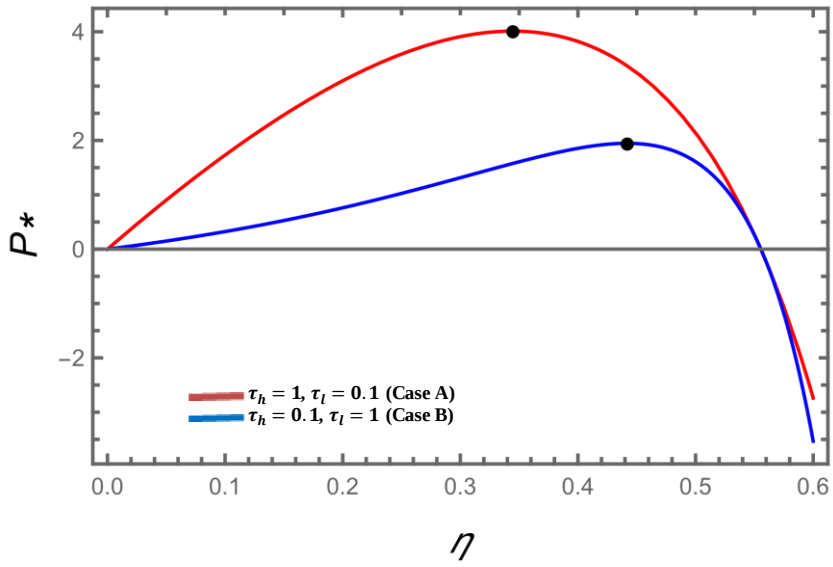

Figure 5. Power as a function of efficiency with different values of isochoric cooling and heating stroke time.

temperature, the more excited atoms there are. Therefore, A will have a higher power than B, even though their total isochoric times are the same. From this result, we get the trade-off between efficiency and power. An engine with high efficiency does not guarantee to produce high power, and an engine with low efficiency mostly produces higher power.

4. CONCLUSION

The result has shown that efficiency at maximum power (EMP) of a quantum Otto engine using BEC does not significantly decline with increasing stroke time when heating and cooling stroke times are equated. This is because the entropy production during the heating process is balanced by the entropy production during the cooling process. However, at different heating and cooling stroke time values, EMP could significantly improve or decline. Due to entropy production and the coherence effect, EMP is low at long heating stroke times and short cooling stroke times but boosted at short heating stroke times and long cooling stroke times. Despite higher EMP, the power of short heating stroke time and long cooling stroke time is much less than the power of long heating stroke time and short cooling stroke time. This is because power is generated by the fraction of atoms outside the condensate, which depends on temperature; the higher the temperature, the more excited the atoms are, and the more power is generated. In another case, EMP is related to the coherence effect produced by the fraction of atoms in the condensate state; the more atoms in the condensate, the more coherent the system is; therefore, the higher its EMP. Nevertheless, another feature of such interaction is that it lends finite compressibility to BEC because the work could be produced from the atoms in the condensate; this issue is left for further investigation.

ACKNOWLEDGEMENT

This work was financially supported by the Faculty of Mathematics and Natural Science, Universitas Andalas with research grant No. 04/UN.16.03.D/PP/FMIPA/2022.

REFERENCE

Abah, O., Roßnagel, J., Jacob, G., Deffner, S., Schmidt-Kaler, F., Singer, K., & Lutz, E. (2012). Single-ion heat engine at maximum power. *Physical Review Letters*, *109*(20). https://doi.org/10.1103/PhysRevLett.109.203006

Altintas, F. (2019). Comparison of the coupled quantum Carnot and Otto cycles. *Physica A: Statistical Mechanics and Its Applications*, *523*, 40–47. https://doi.org/10.1016/j.physa.2019.01.144

Aveline, D. C., Williams, J. R., Elliott, E. R., Dutenhoffer, C., Kellogg, J. R., Kohel, J. M., Lay, N. E., Oudrhiri, K., Shotwell, R. F., Yu, N., & Thompson, R. J. (2020). Observation of Bose–Einstein condensates in an Earth-orbiting research lab. *Nature*, *582*(7811), 193–197. https://doi.org/10.1038/s41586-020-2346-1

Belfaqih, I. H., Sutantyo, T. E. P., Prayitno, T. B., & Sulaksono, A. (2015). Quantum-Carnot engine for particle confined to 2D symmetric potential well. *AIP Conference Proceedings*, 1677 (1), 040010. https://doi.org/10.1063/1.4930654

Boubakour, M., Fogarty, T., & Busch, T. (2022). *Interaction enhanced quantum heat engine*. http://arxiv.org/abs/2211.03394

Çakmak, B., & Müstecaplloğlu, Ö. E. (2019). Spin quantum heat engines with shortcuts to adiabaticity. *Physical Review E*, *99*(3), 1–10. https://doi.org/10.1103/PhysRevE.99.032108

Çakmak, S., Altintas, F., Gençten, A., & Müstecaplıoğlu, Ö. E. (2017). Irreversible work and internal friction in a quantum Otto cycle of a single arbitrary spin. *European Physical Journal D*, *71*(3), 1–10. https://doi.org/10.1140/epjd/e2017-70443-1

Camati, P. A., Santos, J. F. G., & Serra, R. M. (2019). Coherence effects in the performance of the quantum Otto heat engine. *Physical Review A*, *99*(6), 40–43. https://doi.org/10.1103/PhysRevA.99.062103

Chand, S., Dasgupta, S., & Biswas, A. (2021). Finite-time performance of a single-ion quantum Otto engine. *Physical Review E*, *103*(3), 1–9. https://doi.org/10.1103/PhysRevE.103.032144

Curzon, F. L., & Ahlborn, B. (1975). Efficiency of a Carnot engine at maximum power output. *American Journal of Physics*, *43*(1), 22–24. https://doi.org/10.1119/1.10023

Dann, R., & Kosloff, R. (2020). Quantum signatures in the quantum Carnot cycle. *New Journal of Physics*, *22*(1). https://doi.org/10.1088/1367-2630/ab6876

Deffner, S. (2018). Efficiency of harmonic quantum Otto engines at maximum power. *Entropy*, *20*(11). https://doi.org/10.3390/e20110875

Deffner, S., & Campbell, S. (2019). *Quantum Thermodynamics*. Morgan & Claypool Publishers. https://doi.org/10.1088/2053-2571/ab21c6

Donley, E. A., Claussen, N. R., Thompson, S. T., & Wieman, C. E. (2008). Atom-molecule coherence in a bose-einstein condensate. *Collected Papers of Carl Wieman*, 621–625. https://doi.org/10.1142/9789812813787_0085

Fahriza, A., & Sutantyo, T. E. P. (2022). Effects of State Degeneration in 3D Quantum Lenoir Engine Performance. *Jurnal Ilmu Fisika | Universitas Andalas*, *14*(2), 95–107. https://doi.org/10.25077/jif.14.2.95-107.2022

Fahriza, A., Sutantyo, T. E. P., & Abdullah, Z. (2022). Optimizations of multilevel quantum engine with N noninteracting fermions based on Lenoir cycle. *European Physical Journal Plus*, *137*(9). https://doi.org/10.1140/epjp/s13360-022-03235-z

Fei, Z., Chen, J. F., & Ma, Y. H. (2022). Efficiency statistics of a quantum Otto cycle. *Physical Review A*, *105*(2). https://doi.org/10.1103/PhysRevA.105.022609

Griffiths, D. J., & Schroeter, D. F. (2018). *Introduction to Quantum Mechanics*. Cambridge University Press. https://doi.org/10.1017/9781316995433

Jiao, G., Zhu, S., He, J., Ma, Y., & Wang, J. (2021). Fluctuations in irreversible quantum Otto engines. *Physical Review E*, *103*(3), 1–9. https://doi.org/10.1103/PhysRevE.103.032130

Kaushik, S. C., & Kumar, S. (2000). Finite time thermodynamic analysis of endoreversible stirling heat engine with regenerative losses. *Energy*, *25*(10). https://doi.org/10.1016/S0360-5442(00)00023-2

Kim, J., Oh, S., Yang, D., Kim, J., Lee, M., & An, K. (2022). A photonic quantum engine driven by superradiance. *Nature Photonics*, *16*(10), 707–711. https://doi.org/10.1038/s41566-022-01039-2

Kosloff, R., & Rezek, Y. (2017). The Quantum Harmonic Otto Cycle. *Entropy*, *19*(4), 136. https://doi.org/10.3390/e19040136

Meng, Z., Chen, L., & Wu, F. (2020). Optimal power and efficiency of multi-stage endoreversible quantum carnot heat engine with harmonic oscillators at the classical limit. *Entropy*, *22*(4). https://doi.org/10.3390/E22040457

Myers, N. M., Abah, O., & Deffner, S. (2022). *Quantum thermodynamic devices: from theoretical proposals to experimental reality*. https://doi.org/10.1116/5.0083192

Myers, N. M., & Deffner, S. (2020). Bosons outperform fermions: The thermodynamic advantage of symmetry. *Physical Review E*, *101*(1). https://doi.org/10.1103/PhysRevE.101.012110

Myers, N. M., Peña, F. J., Negrete, O., Vargas, P., De Chiara, G., & Deffner, S. (2022). Boosting engine performance with Bose-Einstein condensation. *New Journal of Physics*, *24*(2). https://doi.org/10.1088/1367-2630/ac47cc

Niedenzu, W., Mukherjee, V., Ghosh, A., Kofman, A. G., & Kurizki, G. (2018). Quantum engine efficiency bound beyond the second law of thermodynamics. *Nature Communications*, *9*(1). https://doi.org/10.1038/s41467-017-01991-6

Pathria, R. K., & Beale, P. D. (2011). Statistical Mechanics. In *Statistical Mechanics*. https://doi.org/10.1016/C2009-0-62310-2

Peña, F. J., Myers, N. M., Órdenes, D., Albarrán-Arriagada, F., & Vargas, P. (2023). Enhanced Efficiency at Maximum Power in a Fock–Darwin Model Quantum Dot Engine. *Entropy*, *25*(3), 518. https://doi.org/10.3390/e25030518

Pitaevskii, Lev, and S. S. (2016). *Bose-Einstein condensation and superfluidity*. Oxford University Press.

Reppy, J. D., Crooker, B. C., Hebral, B., Corwin, A. D., He, J., & Zassenhaus, G. M. (2000). Density dependence of the transition temperature in a homogeneous bose-einstein condensate. *Physical Review Letters*, *84*(10), 2060–2063.

https://doi.org/10.1103/PhysRevLett.84.2060
Scovil, H. E. D., & Schulz-Dubois, E. O. (1959). Three-level masers as heat engines. *Physical Review Letters*, *2*(6), 262–263. https://doi.org/10.1103/PhysRevLett.2.262
Scully, M. O., Suhail Zubairy, M., Agarwal, G. S., & Walther, H. (2003). Extracting work from a single heat bath via vanishing quantum coherence. *Science*, *299*(5608). https://doi.org/10.1126/science.1078955
Shen, X., Chen, L., Ge, Y., & Sun, F. (2017). International Journal of Energy And Environment Finite-time thermodynamic analysis for endoreversible Lenoir cycle coupled to constant-temperature heat reservoirs. *Journal Homepage: Www.IJEE.IEEFoundation.Org ISSN*, *8*(3), 2076–2909. www.IJEE.IEEFoundation.org
Smith, Z., Pal, P. S., & Deffner, S. (2020). Endoreversible Otto Engines at Maximum Power. *Journal of Non-Equilibrium Thermodynamics*, *45*(3), 305–310. https://doi.org/10.1515/jnet-2020-0039
Sutantyo, T. E. P. (2020). Three-State Quantum Heat Engine Based on Carnot Cycle. *Jurnal Fisika Unand*, *9*(1), 142–149. https://doi.org/10.25077/jfu.9.1.142-149.2020
Sutantyo, T. E. P., Belfaqih, I. H., & Prayitno, T. B. (2015). Quantum-Carnot engine for particle confined to cubic potential. *AIP Conference Proceedings*, 1677 (1), 040011. https://doi.org/10.1063/1.4930655
Wang, R., Chen, L., Ge, Y., & Feng, H. (2021). Optimizing power and thermal efficiency of an irreversible variable-temperature heat reservoir lenoir cycle. *Applied Sciences (Switzerland)*, *11*(15). https://doi.org/10.3390/app11157171
Yin, Y., Chen, L., Wu, F., & Ge, Y. (2020). Work output and thermal efficiency of an endoreversible entangled quantum Stirling engine with one dimensional isotropic Heisenberg model. *Physica A: Statistical Mechanics and Its Applications*, *547*, 123856. https://doi.org/10.1016/j.physa.2019.123856
Zettili, N., & Zahed, I. (2003). Quantum Mechanics: Concepts and Applications. *American Journal of Physics*, *71*(1), 93–93. https://doi.org/10.1119/1.1522702
Zettira, Z., Fahriza, A., Abdullah, Z., & Sutantyo, T. E. P. (2023). *Enhancing Quantum Otto Engine Performance in Generalized External Potential on Bose-Einstein Condensation Regime*. 1–14. http://arxiv.org/abs/2307.01805